Long-range chemical signalling *in vivo* is regulated by mechanical signals

Eva K. Pillai[1,2,3,#,*], Sudipta Mukherjee[1,#], Niklas Gampl[4,5], Ross J. McGinn[1,4,5,6], Katrin A. Mooslehner[1,4,5], Amelia J. Thompson[1], & Kristian Franze[1,4,5,*]

[1] Department of Physiology, Development and Neuroscience, University of Cambridge, Downing Street, CB2 3DY, Cambridge, United Kingdom

[2] Cell Biology and Biophysics Unit, European Molecular Biology Laboratory, Meyerhofstraße 1, 69117, Heidelberg, Germany

[3] Developmental Biology Unit, European Molecular Biology Laboratory, Meyerhofstraße 1, 69117, Heidelberg, Germany

[4] Institute of Medical Physics and Microtissue Engineering, Friedrich-Alexander-Universität Erlangen-Nürnberg, Henkestraße 91, 91052 Erlangen, Germany

[5] Max-Planck-Zentrum für Physik und Medizin, Kussmaulallee 2, 91054 Erlangen, Germany

[6] Wellcome-MRC Cambridge Stem Cell Institute, Jeffrey Cheah Biomedical Centre, Puddicombe Way, Cambridge Biomedical Campus, CB2 0AW

# These authors contributed equally to this work.

* Correspondence: Eva K. Pillai: eva.pillai@embl.de , phone: +49 6221 3878720

Kristian Franze: kristian.franze@fau.de , phone: +49 9131 8522310

Summary

Biological processes are regulated by chemical signals (e.g., morphogens, growth factors, and guidance cues) and mechanical signals (e.g., tissue stiffness and cellular forces). Yet, the interaction between these two signals *in vivo* remains poorly understood. Using the developing *Xenopus laevis* brain as a model system, where growing retinal ganglion cell (RGC) axons are guided by both chemical and mechanical cues, we demonstrate that knockdown of the mechanosensitive ion channel, Piezo1, exerts cell-intrinsic and cell-extrinsic effects on axon pathfinding. Targeted Piezo1 knockdown in RGCs led to pathfinding errors *in vivo.* However, pathfinding errors were also observed in RGCs expressing Piezo1, when Piezo1 was downregulated in the surrounding brain tissue. Depleting Piezo1 levels led to both a decrease in the expression of the long-range chemical guidance cues, Semaphorin3A (Sema3A) and Slit1, and a decrease in tissue stiffness. While tissue softening was independent of Sema3A depletion, Slit1 and Sema3A expression increased significantly in stiffer environments *in vitro*. Moreover, stiffening soft brain regions *in vivo* induced ectopic production of Sema3A, via a Piezo1-dependent mechanism. Our results show that brain tissue mechanics modulates the expression of key chemical cues. This dynamic interplay between tissue mechanics and long-range chemical signalling likely extends across diverse biological systems throughout development, homeostasis, and disease.

Keywords: *Tissue mechanics; Chemical guidance cues; Axon pathfinding; Piezo1; Semaphorin3A; Slit1; Mechanobiology; Mechanotransduction; Forces; Stiffness.*

Numerous cellular and tissue-level processes in biology are regulated by long-range concentration gradients of diffusible chemical signals, which act in concert to spatio-temporally control the function of cells within tissues[1]. Morphogen gradients, for example, set positional information during organismal development[2–6], while growth factor and hormone gradients are essential for organ development and maintenance[7]. Signalling molecules often have multitudinous functions; for instance, the Semaphorin family of proteins regulate cell morphology and motility in the nervous, immune, respiratory, cardiovascular, and musculoskeletal systems during development, homeostasis, and disease[8]. Similarly, Slit proteins play important roles in brain, kidney, heart, and mammary gland development, as well as in various disease states, by regulating cell proliferation, migration, vascularization and more[9].

Recent work demonstrated that many of these cellular functions are also regulated by tissue mechanics. For instance, mechanical anisotropies in tissues affect growth orientation, while factors such as mechanical stresses, environmental stiffness, and cell or tissue geometry profoundly affect cell proliferation, migration, and fate specification[10–12]. In the nervous system, for example, mechanical forces regulate development and various physiological processes, while alterations in tissue mechanics occur in neurodegenerative diseases and other pathophysiological conditions[13]. Thus, besides the well-established role of chemical signals, mechanical cues have recently emerged as equally critical regulators of biological processes.

Indeed, cells will always be simultaneously exposed to both chemical and mechanical cues. One example is the extension of neuronal axons along precise paths during nervous system development, termed axon pathfinding. In the *Xenopus laevis* optic pathway, retinal

ganglion cell (RGC) axons exhibit a stereotypical trajectory, exiting the eye via the optic nerve, crossing the midline at the optic chiasm, traversing the contralateral brain surface, and making a characteristic caudal turn at the mid-diencephalon before reaching their target, the optic tectum[14,15] (Fig. 1a). Several membrane-bound and diffusible signalling molecules pattern the surrounding brain tissue, directing *Xenopus* RGC axons along this specific path[16]. For instance, the caudal turn of RGC axons in the mid-diencephalon is regulated by gradients of the repulsive long-range guidance cues, Slit1[17] and Semaphorin3A (Sema3A)[18]. At the same time, RGC axons are mechanosensitive and encounter an instructive stiffness gradient in the brain, which also contributes to regulating RGC axon pathfinding in that region[19,20]. However, the interaction between chemical and mechanical signalling *in vivo* remains elusive.

A key player involved in sensing and responding to brain tissue stiffness[19,21] is the mechanosensitive nonselective cation channel Piezo1[22,23]. Piezo1 is found in a broad range of animal tissues including the bladder, kidneys, lung, and skin[22], as well as in the developing *Xenopus* nervous system[19,24]. Downregulating Piezo1 expression in the nervous system *in vivo* leads to aberrant axon growth and severe pathfinding defects during development[19]. To disentangle the effect of Piezo1 activity in RGC axons from that of the surrounding neuroepithelial cells on axon pathfinding, we selectively downregulated Piezo1 in the axons while preserving its expression in the surrounding brain tissue. This targeted depletion was achieved by injecting translation-blocking morpholinos into one of the two dorsal blastomeres at the 4-cell stage, resulting in embryos with Piezo1 depletion in one half of the nervous system. As RGC axons cross over completely in the *Xenopus* optic chiasm to the contralateral brain surface[25], this approach yielded embryos with Piezo1-depleted RGC axons growing across normal brain tissue and, in the contralateral brain hemisphere, normal

RGC axons growing across Piezo1-depleted brain tissue (Fig. 1b). RGC axons were labelled with DiI, and their trajectories analysed at developmental stage 40[26], when axons had reached their end target, the optic tectum.

Consistent with our previous findings[19], simultaneous downregulation of Piezo1 in both axons and the surrounding brain tissue led to severe axon pathfinding defects (Fig. 1c,f), compared with age-matched sibling embryos, where both dorsal blastomeres were injected with a control morpholino. The elongation of the RGC axon bundle growing along the brain surface, or optic tract, was significantly lower than in controls ($p = 0.002$, Kruskal-Wallis with Dunn post-hoc test) (Fig. 1g). Furthermore, only 13% of brains had normal axonal projections, while 61% of brains exhibited stalling and/or misprojection defects (i.e., deviations from the normal trajectory, such as bypassing the caudal turn in the mid-diencephalon or misrouting dorso-anteriorly into the telencephalon) (Fig. 1h). Representative images illustrating normal RGC axonal projections and various axon guidance defects are shown in Supplementary Fig. 1.

When Piezo1 was selectively depleted in RGC axons (Fig. 1d), optic tract elongation was similar as in controls ($p > 0.999$, Kruskal-Wallis with Dunn post-hoc test, Fig. 1g). Nonetheless, only 44% of these brains exhibited normal axonal projections (Fig. 1h). Piezo1 downregulation in the axons resulted in 28% of brains with stalling defects, while 44% of the brains showed misprojecting or both stalling and misprojecting defects (Fig. 1h). These results confirmed that RGC axons probe their mechanical environment via Piezo1, and that this cell-intrinsic mechanosensing is required for accurate pathfinding. However, the overall phenotype was milder than what we had observed in brains with downregulated Piezo1 expression in both RGC axons and the surrounding neuroepithelium[19] (Fig. 1f-h), suggesting

that Piezo1 expression in neuroepithelial cells was also required for proper axon pathfinding.

Indeed, when Piezo1 downregulation was limited to the surrounding brain tissue, axon pathfinding of healthy RGCs containing Piezo1 was also perturbed. In fact, the observed guidance defects were even more profound than in the brains with axonal Piezo1 knockdown (Fig. 1e). Optic tract elongation was significantly decreased if compared to controls ($p = 0.010$, Kruskal-Wallis with Dunn post-hoc test) (Fig. 1g), and only 38% of brains showed normal axonal projections. In contrast, 56% of brains exhibited stalling and/or splaying and misprojecting axons (Fig. 1h). Thus, despite normal Piezo1 levels in RGC axons, axon growth patterns were disrupted, confirming that Piezo1-mediated mechanosensing by neuroepithelial cells was also essential for accurate axon pathfinding.

We next investigated how perturbations of neuroepithelial mechanosensing may lead to disruptions in growth patterns of healthy axons. At least two RGC-extrinsic factors are crucial for the turning of the optic tract in the mid-diencephalon (Fig. 1a): local tissue stiffness[19] and long-range chemical signalling by the repulsive guidance cues Slit1[17] and Semaphorin3A (Sema3A)[18], which are both located rostrally to the optic tract's caudal turn (Fig. 2a,e). Chemical perturbations of brain tissue stiffness *in vivo* mostly lead to a splaying of RGC axons in the diencephalon[19], while depletion of Slit1 and Sema3A signalling dominantly leads to a stalled axon phenotype[17,27]. Since we found both axon guidance defects after downregulating Piezo1 expression in neuroepithelial cells (Fig. 1e,h), we first tested the effect of Piezo1 downregulation on the expression of these chemical guidance cues using hybridization chain reaction-fluorescence in situ hybridization (HCR-FISH).

In stage 40 control-injected sibling embryos, our HCR-FISH results recapitulate published *in situ* hybridization data[17,18,28]: Slit1 forms a distinct band between the telencephalon and diencephalon, while Sema3A is highly expressed rostro-ventrally of Slit1 in the telencephalon (Fig. 2b,f). Piezo1 downregulation resulted in a significantly smaller area occupied by Slit1 ($p = 0.004$, unpaired t-test with Welch's correction) (Fig. 2c,d), and Sema3A mRNA expression was significantly decreased compared to controls ($p = 0.025$, unpaired t-test with Welch's correction) (Fig. 2g,h). Standard *in situ* hybridizations confirmed the dramatic decrease in Sema3A mRNA expression in Piezo1-depleted brain tissue (Fig. 2 i,j). Additionally, Western blot analysis confirmed that Piezo1 downregulation resulted in significant decreases in Sema3A ($p = 0.003$, ratio paired t-test) (Fig. 2k,l) and Piezo1 protein levels, but not in the housekeeping protein b-actin, (Fig. 2k and Supplementary Fig. 2); Slit1 protein expression could not be assessed due to a lack of suitable antibodies in *Xenopus*. Hence, our data indicated that the downregulation of Piezo1 – a mechanosensor – in neuroepithelial cells attenuated the expression of key chemical cues, implying a role for mechanical signalling in modulating chemical signalling during development.

The splaying of axons seen in Piezo1-downregulated brain parenchyma (Fig. 1e,f) recapitulated the phenotype of RGC axons growing through brain tissue that was chemically softened *in vivo*[19]. In order to test if, in addition to the chemical landscape, tissue mechanics was also altered in Piezo1 knockdown brains, we employed atomic force microscopy (AFM)-based stiffness mapping[19,20] to measure the stiffness of live developing *Xenopus* brains at stage 40. Tissue stiffness was quantified by the reduced apparent elastic modulus, K, whereby a larger K value indicates stiffer tissue. Measurements were performed *in vivo* in a rectangular grid on the exposed brain surface (Fig. 3a,b) of stage-matched sibling embryos for control

injected embryos and embryos in which Piezo1 was downregulated either exclusively in the axons or in the surrounding brain tissue, or in both.

The overall mechanical landscape of brains with Piezo1-downregulation in solely the RGC axons was similar to that of control embryos (median K_{ctrl} = 432 Pa, $K_{Axon\ k/d}$ = 467 Pa; $p > 0.999$, Kruskal-Wallis with Dunn post-hoc test) (Fig. 3c,d), suggesting that the observed axon pathfinding defects shown in Fig. 1d were not a consequence of alterations in tissue stiffness but rather originated in the axons' reduced ability to sense their mechanical environment. Conversely, downregulating Piezo1 either exclusively in the surrounding brain tissue or simultaneously in the axons and surrounding brain tissue resulted in a close to two-fold decrease in brain stiffness (median $K_{Brain\ k/d}$ = 231 Pa, $K_{Double\ k/d}$ = 240 Pa; $p < 0.0001$, Kruskal-Wallis with Dunn post-hoc test) (Fig. 3c,d). Hence, the knockdown of Piezo1 in the developing neuroepithelium led to considerable changes in both the chemical and mechanical landscape encountered by growing RGC axons.

We then wanted to know whether there was a causal relationship between the decrease in guidance cue expression (Fig. 2) and the decrease in tissue stiffness (Fig. 3c,d) in Piezo1 knockdown brains. In particular, we asked if tissue softening was a consequence of the decrease in Sema3A and Slit1, or if, vice versa, the decrease in guidance cue expression was a consequence of the change in tissue stiffness. Given the spatially restricted expression of Slit1 mRNA and the uncertainty if protein levels had changed after Piezo1 knockdown, we here focused on the effect of Sema3A depletion on tissue stiffness.

To downregulate endogenous Sema3A protein in the brain without altering the early developmental expression of Piezo1 levels, we electroporated the forebrain of stage 29/30 embryos with either a Sema3A or a control fluorescein-tagged morpholino[27]. The

electroporated embryos were allowed to develop to stage 40, at which point tissue stiffness was measured using AFM (Fig. 3e). Downregulating Sema3A protein expression in the forebrain did not result in brain tissue softening. In fact, the stiffness of the Sema3A-depleted forebrain region increased compared to controls, with a median K = 455 Pa in the Sema3A knockdown brain and K = 350 Pa in the control ($p < 0.0001$, Wilcoxon rank-sum test) (Fig. 3f,g), while brain tissue mechanics in adjacent regions was unaltered in these embryos (median $K_{Sema3A\ k/d}$ = 332 Pa, K_{ctrl} = 341 Pa; $p = 0.67$, Wilcoxon rank-sum test) (Fig 3h). These data showed that the observed stiffening was specific to the localized Sema3A depletion, and suggested that the decrease in guidance cues in Piezo1 knockdown brains is likely not responsible for the decrease in tissue stiffness.

To test if, instead, tissue stiffness may modulate chemical guidance cue expression, independently of the decrease in Piezo1 expression, we first exposed brain tissue to different mechanical environments and measured their effect on the expression of Slit1 and Sema3A mRNA using HCR-FISH. Brain tissues of wild type embryos at stage 37/38, at which point axons already respond to Sema3A[18] and Slit1, was harvested from stiff brain regions[19] that produce the guidance cues (telencephalon) and from the adjacent soft brain region[19] that typically does not (hypothalamus) (Fig. 4a). Both tissue types were separately embedded in soft (40 Pa) and stiff (450 Pa) 3D hydrogels (Fig. 4a)[29]. Cells at the edges of the tissue regions embedded in the substrates pulled on the surrounding hydrogel with forces on the order of ~50 nN, visibly deforming the material and thus probing its mechanical properties (Supplementary Fig. 3; Supplementary movie 1). After 24 hours in culture, Slit1 and Sema3A expression in telencephalic tissue was independent of the environmental stiffness ($p_{Slit1} = 0.824$, $p_{Sema3A} = 0.542$, ratio paired t-test) (Supplementary Fig. 4). However, in hypothalamic tissue, we found a significant increase in both Slit1 and Sema3A mRNA

expression in stiff compared to soft substrates (p_{Slit1} = 0.025, p_{Sema3A} = 0.050, ratio paired t-test) (Fig. 4b-e), suggesting that altering environmental mechanics may modulate the expression of chemical guidance cues in soft brain tissues *in vitro*.

To corroborate the effect of tissue stiffness on the expression of long-range chemical signals *in vivo*, we used AFM-based compression stiffening[19,30] to locally stiffen stage 35/36 soft hypothalamic brain regions, for > 6 hours (until embryos reached stage 40) *in vivo* and subsequently assessed mRNA expression with HCR-FISH (Fig. 4f). Slit1 expression was not significantly different from controls in compression-stiffened brains (p = 0.169, unpaired t-test with Welch's correction) (Supplementary Fig. 5). However, in line with our *in vitro* data (Fig. 4e), stiffening the tissue resulted in the ectopic production of the chemical guidance cue Sema3A at the hypothalamus (Fig. 4,h). In compression-stiffened brains, there was a significant increase in mRNA levels compared to controls (p = 0.011, unpaired t-test with Welch's correction) (Fig. 4g-i), indicating that *in vivo* tissue stiffness may indeed regulate the expression of the long-range chemical signal, Sema3A.

Since Piezo1-depleted brains had decreased Sema3A expression (Fig. 2) and were softer than control brains (Fig. 3), and as an increase in tissue stiffness led to an increase in Sema3A expression *in vivo* (Fig. 4g-i), we finally tested if stiffening telencephalic regions, where Sema3A is normally produced, is sufficient to rescue Sema3A expression in Piezo1 knockdown brains (Fig. 4j). Compression-stiffening Piezo1-depleted stage 35/36 brains for > 6 hours did not restore Sema3A levels (p = 0.170, unpaired t-test with Welch's correction) (Fig 4k-m), suggesting that both tissue stiffness and adequate levels of Piezo1, which not only regulates but also detects tissue stiffness, are required to lay down the appropriate chemical landscape for supporting axon pathfinding in the developing brain.

Discussion

During numerous processes in diverse biological systems, including brain development, cells encounter a plethora of chemical and mechanical cues in their environment, which they detect, integrate, and interpret. We here discovered an intricate interplay between mechanical and long-range chemical signalling *in vivo*, with both influencing each other, showing that neither cue can be fully understood in isolation. Collectively, our results underscore a crucial role of Piezo1 in both RGC-intrinsic and cell-extrinsic regulations of axon pathfinding in the developing *Xenopus* retino-tectal system.

We found that the mechanosensitive ion channel, Piezo1, has at least a dual function in the developing brain. On the one hand, it is involved in sensing tissue stiffness[19] (Fig. 1d,h). On the other hand, it inherently contributes to regulating the mechanical properties of the tissue (Fig. 3a-d), and in turn, the appropriate tissue stiffness is required for the expression of long-range chemical guidance cues (Fig. 4). Downregulation of Piezo1 in brain tissues led to a decrease in tissue stiffness (Fig. 3) and a subsequent decrease of the expression of Sema3A and Slit1 (Figs. 2, 4). In contrast, the downregulation of Sema3A was followed by an increase in tissue stiffness (Fig. 3e-h), indicating that feedback mechanisms between tissue stiffness and gene expression levels do not always act reciprocally.

Recent work has shown that softer substrates lead to a decrease in Piezo1 expression levels *in vitro*[31,32]. We here found the converse to also hold true; a decrease in Piezo1 expression leads to tissue softening *in vivo* (Fig. 3), suggesting a positive feedback loop. In line with our data, Piezo1 levels in microglial cells correlate with the stiffness of Aβ plaque-associated brain tissues[33], and in macrophages with the stiffness of ischemic tissues[34]. Furthermore, in *Drosophila*, dPiezo depletion led to softening of gliomas driven by different

oncogenic mutations but not of non-transformed brains[35]. How Piezo1 contributes to the regulation of tissue mechanics remains to be studied. Potential contributions could arise from the impact of its activity on cell proliferation[36,37], on the mechanical properties of cells[38], or on the extracellular matrix composition[39].

In vitro, environmental stiffness affected Sema3A and Slit1 mRNA expression in the hypothalamus but not in telencephalic regions (Supplementary Fig. 4). At stage 37/38, the telencephalon is already stiffer than the adjacent hypothalamus[20] and chemical cues (Slit1 and Sema3A) are already expressed in this region[28]. Thus, exposing this stiff tissue, which is already poised to produce chemical cues, to a stiffer environment *in vitro* may not lead to further alterations in their expression profile.

While increasing tissue stiffness *in vivo* was sufficient to induce ectopic Sema3A expression in soft brain regions of wild type embryos, in Piezo-downregulated brains tissue stiffening did not rescue Sema3A expression (Fig. 4), indicating that Piezo1 in neuroepithelial cells was also required to detect mechanical signals and induce Sema3A expression (Fig. 4). A dependence of Sema3A expression on tissue stiffness is consistent with expression patterns found in healthy *Xenopus* brains. Here, Sema3A is expressed in the telencephalon, which is significantly stiffer than the diencephalon and hypothalamus[19], where Sema3A is not expressed (Fig. 2). However, Sema3A is already expressed in the telencephalon region at stage 32[28] - before the telencephalon stiffens[20] – indicating that other factors contribute to regulating Sema3A.

The expression of both Sema3A and Slit1 is known to be regulated by FGF signalling[17,28]. FGF receptors, however, can be activated in the absence of ligands through mechanical forces[40]. As cellular traction forces are higher in stiffer environments, stiffer tissues could lead to the enhanced activation of FGF receptors, thus facilitating guidance

cue expression in the developing brain even in the absence of FGF. If, for example, FGF levels decrease over time or distance during development, higher Sema3A and Slit1 expression levels could still be maintained via Piezo1-mediated responses to enhanced tissue stiffness (Fig. 4). This would also explain why the expression of Sema3A can be triggered in the brain ectopically through a stiffer environment (Fig. 4c,e) or the external application of a mechanical force (Fig. 4h,i).

Depleting Piezo1 early in development may not only affect tissue stiffness (Fig. 3) but potentially also neural stem/progenitor cell fate determination[21,41] or FGF signalling[42]. Thus, there are several potential pathways how the mechanosensitive ion channel Piezo1 might regulate long-range chemical signalling. Future work will reveal molecular details on how Piezo1 activity is coupled to gene expression profiles of key signalling molecules.

In the developing *Xenopus* brain, Piezo1 is critical for setting up the mechanical and chemical landscape required for proper RGC axon guidance. Our findings raise the intriguing possibility that tissue mechanics may regulate the transcription of many other biochemical factors[43] in various other organ systems – and *vice versa*. Understanding the complex interplay between chemical and mechanical signalling is a challenge but has great potential to provide new insights into the regulation of development, physiology, ageing, and disease.

Methods

Detailed methods are available in the online version of the paper, including the associated code and references.

Data availability

The datasets generated during and/or analysed during the current study are available from the authors on reasonable request.

Acknowledgements

We thank Christine Holt, Maximilian Jakobs, Sarah Foster, Kevin Chalut, and Nick Brown for insightful discussions; Alex Winkel, Liz Williams, and Asha Dwivedy for technical help; Can Aztekin (EPFL Lausanne, Switzerland), Chaitanya Dingare, and Jakub Sedzinski (The Danish Stem Cell Centre, University of Copenhagen, Denmark) for HCR-FISH protocol optimization advice. We also acknowledge the Cambridge Advanced Imaging Centre for support in this work. This work has been funded by a Wellcome Trust PhD studentship 222280/Z/20/Z (S.M.), Cambridge Trust scholarship (S.M.), an MRC Doctoral Training Grant awarded to the Wellcome-MRC Cambridge Stem Cell Institute: MR/R50211X/1 (R.J.M.), a European Research Council Consolidator Award 772426 (K.F.), the German Research Foundation (DFG) projects 460333672 CRC1540 EBM and 270949263 GRK2162 (K.F.) and an Alexander von Humboldt Professorship (Alexander von Humboldt Foundation) (K.F.).

Author contributions

E.K.P., S.M., and K.F., designed the study. E.K.P., S.M., N.G., R.J.M., K.A.M., and A.J.T., carried out experiments, data analysis, data curation and visualization. E.K.P, and K.F., wrote the manuscript. K.F., supervised the study. All authors reviewed and edited the manuscript.

References

1. Kicheva, A. & Briscoe, J. Control of Tissue Development by Morphogens. *Annu. Rev. Cell Dev. Biol.* **39**, 91–121 (2023).

2. Driever, W. & Nüsslein-Volhard, C. The bicoid protein determines position in the Drosophila embryo in a concentration-dependent manner. *Cell* **54**, 95–104 (1988).

3. Strigini, M. & Cohen, S. M. A Hedgehog activity gradient contributes to AP axial patterning of the Drosophila wing. *Development* **124**, 4697–4705 (1997).

4. Chen, Y. & Schier, A. F. The zebrafish Nodal signal Squint functions as a morphogen. *Nature* **411**, 607–610 (2001).

5. Briscoe, J., Chen, Y., Jessell, T. M. & Struhl, G. A Hedgehog-Insensitive Form of Patched Provides Evidence for Direct Long-Range Morphogen Activity of Sonic Hedgehog in the Neural Tube. *Mol. Cell* **7**, 1279–1291 (2001).

6. Lecuit, T. *et al.* Two distinct mechanisms for long-range patterning by Decapentaplegic in the Drosophila wing. *Nature* **381**, 387–393 (1996).

7. Norman, A. W. & Henry, H. L. Growth Factors. in *Hormones* 363–379 (Elsevier, 2015). doi:10.1016/B978-0-08-091906-5.00017-3.

8. Alto, L. T. & Terman, J. R. Semaphorins and their Signaling Mechanisms. in *Methods in Molecular Biology* vol. 1493 1–25 (2017).

9. Blockus, H. & Chédotal, A. Slit-Robo signaling. *Development* **143**, 3037–3044 (2016).

10. LeGoff, L. & Lecuit, T. Mechanical Forces and Growth in Animal Tissues. *Cold Spring Harb. Perspect. Biol.* **8**, a019232 (2016).

11. Heisenberg, C.-P. & Bellaïche, Y. Forces in Tissue Morphogenesis and Patterning. *Cell*

153, 948–962 (2013).

12. Hannezo, E. & Heisenberg, C.-P. Mechanochemical Feedback Loops in Development and Disease. *Cell* **178**, 12–25 (2019).

13. Pillai, E. K. & Franze, K. Mechanics in the nervous system: From development to disease. *Neuron* (2023) doi:10.1016/j.neuron.2023.10.005.

14. Harris, W. A. Homing behaviour of axons in the embryonic vertebrate brain. *Nature* **320**, 266–269 (1986).

15. Holt, C. E. A Single-Cell Analysis of Early Retinal Ganglion Cell Differentiation in Xenopus: From Soma to Axon Tip. *J. Neurosci.* **9**, 3123–3145 (1989).

16. McFarlane, S. & Lom, B. The Xenopus retinal ganglion cell as a model neuron to study the establishment of neuronal connectivity. *Dev. Neurobiol.* **72**, 520–36 (2012).

17. Atkinson-Leadbeater, K. *et al.* Dynamic Expression of Axon Guidance Cues Required for Optic Tract Development Is Controlled by Fibroblast Growth Factor Signaling. *J. Neurosci.* **30**, 685–693 (2010).

18. Campbell, D. S. *et al.* Semaphorin 3A elicits stage-dependent collapse, turning, and branching in Xenopus retinal growth cones. *J. Neurosci.* **21**, 8538–47 (2001).

19. Koser, D. E. *et al.* Mechanosensing is critical for axon growth in the developing brain. *Nat. Neurosci.* **19**, 1592–1598 (2016).

20. Thompson, A. J. *et al.* Rapid changes in tissue mechanics regulate cell behaviour in the developing embryonic brain. *Elife* **8**, (2019).

21. Pathak, M. M. *et al.* Stretch-activated ion channel Piezo1 directs lineage choice in human neural stem cells. *Proc. Natl. Acad. Sci. U. S. A.* **111**, 16148–53 (2014).

22. Coste, B. *et al.* Piezo1 and Piezo2 Are Essential Components of Distinct Mechanically Activated Cation Channels. *Science (80-.).* **330**, 55–60 (2010).

23. Coste, B. *et al.* Piezo proteins are pore-forming subunits of mechanically activated channels. *Nature* **483**, 176–81 (2012).

24. Session, A. M. *et al.* Genome evolution in the allotetraploid frog Xenopus laevis. *Nature* **538**, (2016).

25. Nakagawa, S. *et al.* Ephrin-B regulates the Ipsilateral routing of retinal axons at the optic chiasm. *Neuron* **25**, 599–610 (2000).

26. Nieuwkoop, P. D. & Faber, J. Normal Table of Xenopus Laevis (Daudin). *Copeia* **1958**, (1958).

27. Leung, L. C. *et al.* Coupling of NF-protocadherin signaling to axon guidance by cue-induced translation. *Nat. Neurosci.* **16**, 166–173 (2013).

28. Yang, J. L. J., Bertolesi, G. E., Dueck, S., Hehr, C. L. & McFarlane, S. The expression of key guidance genes at a forebrain axon turning point is maintained by distinct fgfr isoforms but a common downstream signal transduction mechanism. *eNeuro* **6**, (2019).

29. Böhringer, D. *et al.* Dynamic traction force measurements of migrating immune cells in 3D matrices. *bioRxiv* 2022.11.16.516758 (2023) doi:10.1101/2022.11.16.516758.

30. Barriga, E. H., Franze, K., Charras, G. & Mayor, R. Tissue stiffening coordinates morphogenesis by triggering collective cell migration in vivo. *Nature* **554**, 523–527 (2018).

31. Li, M. *et al.* Activation of Piezo1 contributes to matrix stiffness-induced angiogenesis

in hepatocellular carcinoma. *Cancer Commun.* **42**, 1162–1184 (2022).

32. Atcha, H. *et al.* Mechanically activated ion channel Piezo1 modulates macrophage polarization and stiffness sensing. *Nat. Commun.* **12**, 3256 (2021).

33. Hu, J. *et al.* Microglial Piezo1 senses Aβ fibril stiffness to restrict Alzheimer's disease. *Neuron* **111**, 15-29.e8 (2023).

34. Xie, L. *et al.* Piezo1 (Piezo-Type Mechanosensitive Ion Channel Component 1)-Mediated Mechanosensation in Macrophages Impairs Perfusion Recovery After Hindlimb Ischemia in Mice. *Arterioscler. Thromb. Vasc. Biol.* **43**, 504–518 (2023).

35. Chen, X. *et al.* A Feedforward Mechanism Mediated by Mechanosensitive Ion Channel PIEZO1 and Tissue Mechanics Promotes Glioma Aggression. *Neuron* **100**, 799-815.e7 (2018).

36. Gudipaty, S. A. *et al.* Mechanical stretch triggers rapid epithelial cell division through Piezo1. *Nature* **543**, 118–121 (2017).

37. Segel, M. *et al.* Niche stiffness underlies the ageing of central nervous system progenitor cells. *Nature* **573**, 130–134 (2019).

38. Emig, R. *et al.* Piezo1 Channels Contribute to the Regulation of Human Atrial Fibroblast Mechanical Properties and Matrix Stiffness Sensing. *Cells* **10**, 663 (2021).

39. Wang, L. *et al.* Mechanical sensing protein PIEZO1 regulates bone homeostasis via osteoblast-osteoclast crosstalk. *Nat. Commun.* **11**, 282 (2020).

40. Kinoshita, N. *et al.* Mechanical Stress Regulates Epithelial Tissue Integrity and Stiffness through the FGFR/Erk2 Signaling Pathway during Embryogenesis. *Cell Rep.* **30**, 3875-3888.e3 (2020).

41. Nourse, J. L. *et al.* Piezo1 regulates cholesterol biosynthesis to influence neural stem cell fate during brain development. *J. Gen. Physiol.* **154**, (2022).

42. Wang, S. *et al.* Adipocyte Piezo1 mediates obesogenic adipogenesis through the FGF1/FGFR1 signaling pathway in mice. *Nat. Commun.* **11**, 2303 (2020).

43. Sipkova, J. & Franze, K. Eph/ephrin signalling in the developing brain is regulated by tissue stiffness. *bioRxiv* (2024).

Figures

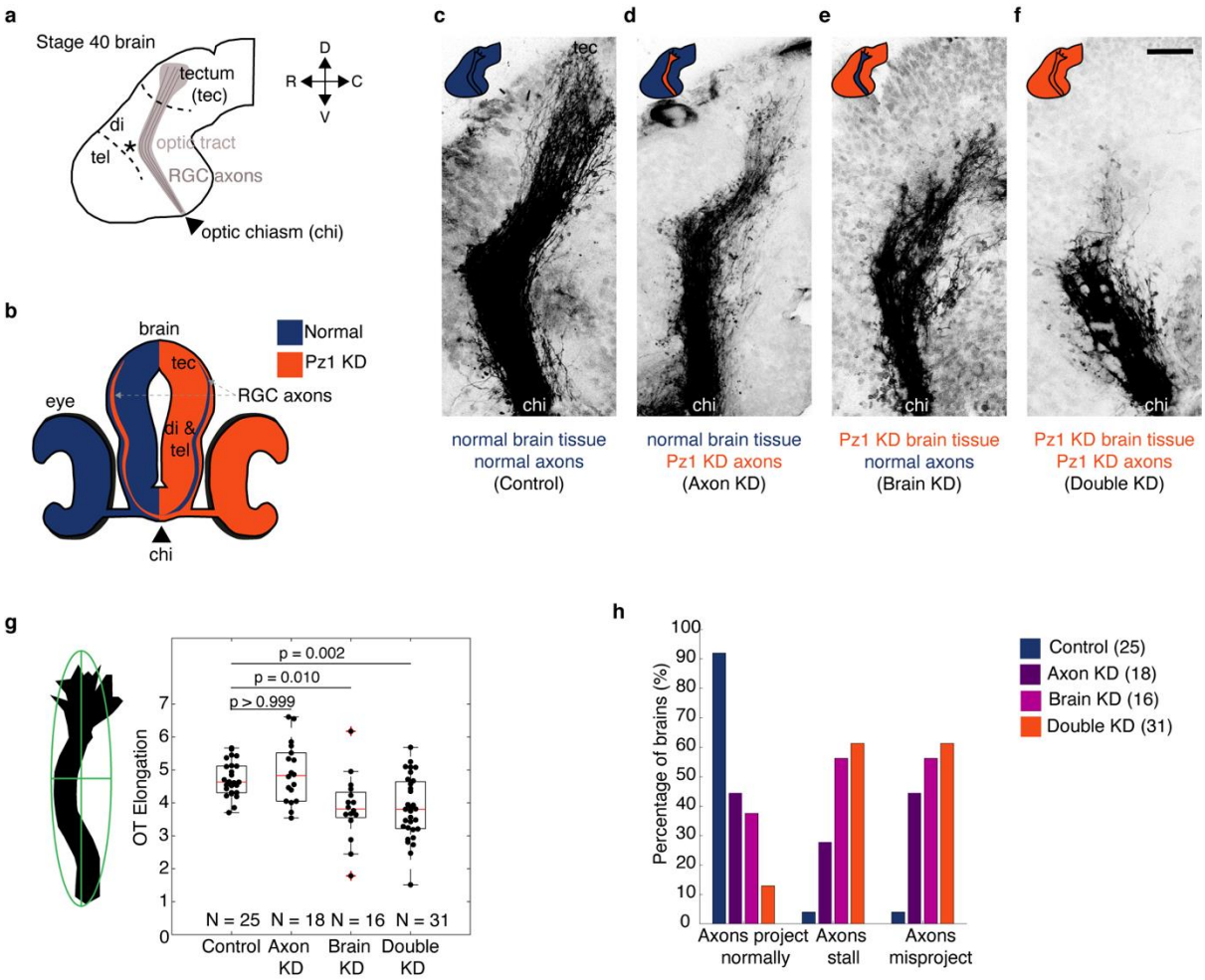

Figure1: RGC intrinsic and extrinsic Piezo1 signalling is required for accurate axon pathfinding *in vivo*. a, Schematic of the lateral view of a stage 40 *Xenopus* brain with orientation guides for Rostral-Caudal (R, C) and Dorsal-Ventral (D,V) axes. RGC axons grow from the optic chiasm towards the optic tectum along a stereotypic path (the optic tract), turning caudally at the mid-diencephalon ("*"). **b,** Schematic cross-section of a Xenopus brain and retinae when Piezo1 is downregulated unilaterally in the nervous system. RGC axons cross the midline at the optic chiasm and grow across the contralateral brain surface. Normal Piezo1 levels are indicated in blue while Piezo1 depletion is shown in red. Piezo1-depleted axons grow across brain tissue with normal Piezo1 levels and *vice-versa*. **c-f,**

Images of RGC axon growth *in vivo*. Axon growth and guidance were affected by downregulating Piezo1 (**d)** in the axons, (**e**) in the surrounding brain tissue, or (**f**) in both. Scale bar: 50 µm. **g,** Optic tract elongation, the ratio of long to short axes on a fitted ellipse (schematic), decreased significantly when Piezo1 was downregulated in the brain parenchyma. Each point represents a brain. Boxplots show median, first, and third quartiles; whiskers show the spread of data; '+' indicate outliers. N denotes the number of animals. Data were assessed with a Kruskal-Wallis test, $p < 0.0001$, and with a Dunn post-hoc test (adjusted p-values provided in the figure). **h,** Scoring of brains displaying aberrant phenotypes. Knocking down Piezo1 solely in the axons or brain tissue, or in both, result in significant stalling/misprojecting defects (Fisher's exact test, $p < 0.0001$, number of animals in parentheses). di: diencephalon, chi: chiasm, KD: knockdown, Pz1: Piezo1, RGC: retinal ganglion cell, tec: tectum, tel: telencephalon.

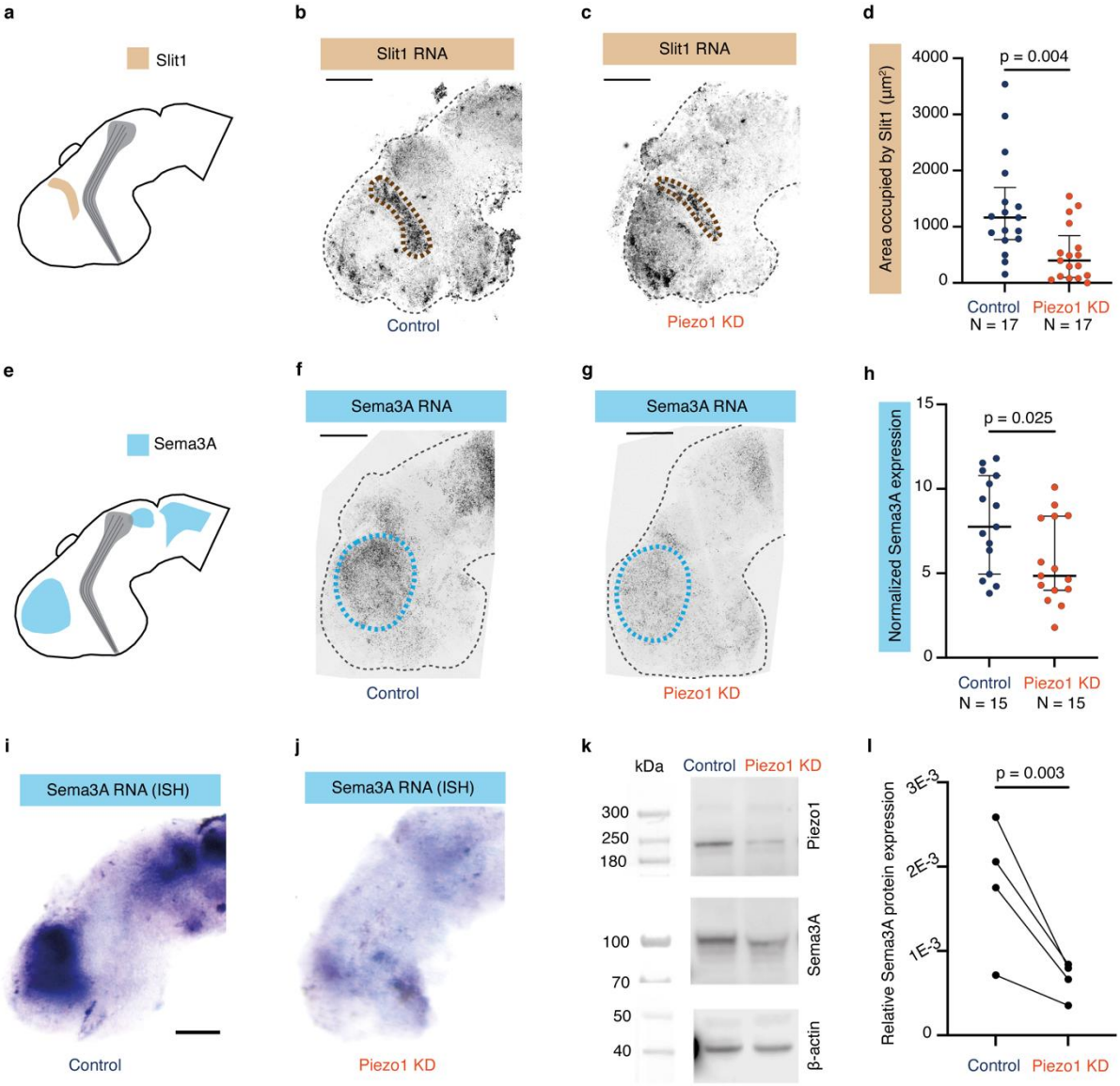

Figure 2: Piezo1 downregulation attenuates the expression of long-range chemical guidance cues *in vivo*. a, Schematic representation of the expression pattern of the chemical guidance cue, Slit1. **b-c,** Representative hybridization chain reaction-fluorescence *in situ* hybridisation (HCR-FISH) images of Slit1 expression in (**b**) a control and (**c**) a Piezo1 knockdown brain. **d,** Quantification of Slit1 mRNA distributions. Slit1 occupied a significantly smaller area in Piezo1 knockdown brains compared to control brains. **e,** Schematic of the expression pattern of Sema3A. **f-g,** Representative HCR-FISH images of Sema3A expression in (**f**) a control and (**g**) in a Piezo1 knockdown brain. **h,** Quantification of normalized Sema3A

expression. Sema3A expression decreased significantly when Piezo1 was downregulated. **i-j,** *In situ* hybridisation of Sema3A mRNA expression, confirming a dramatic attenuation of the Sema3A signal in Piezo1 knockdown brains (**j**) compared to controls (**i**). **k,** Western blot image of Piezo1, Sema3A and β -actin protein expression in control and Piezo1-depleted brains. **l,** Western blot quantification. Downregulating Piezo1 led to significantly decreased Sema3A protein expression. Each point in **d** & **h** represents an embryo, lower quartile, median, and upper quartiles are indicated. N denotes the number of animals. Data in **d** & **h** were assessed with an unpaired t-test with Welch's correction. Each point in **l** indicates the mean value of a biological replicate. Data in **l** was assessed with a ratio paired t-test. p-values shown in the figures. Scale bars: 100 µm. ISH: *In situ* hybridisation, KD: knockdown.

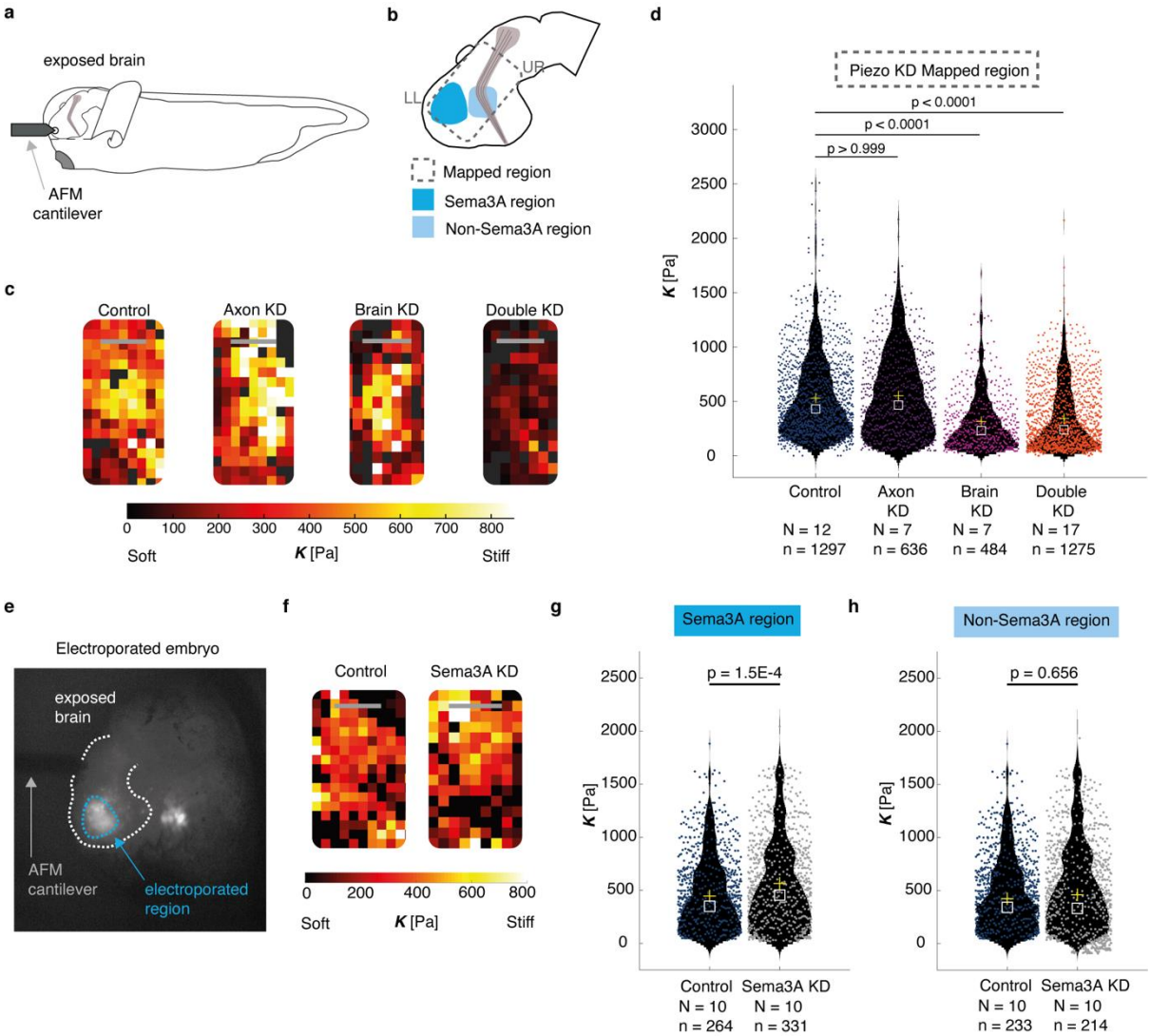

Figure 3: Piezo1, but not Sema3A, knockdown leads to brain tissue softening. a, Schematic of the experimental setup for *in vivo* brain-stiffness mapping. **b,** *Xenopus* brain schematics. The dashed rectangle indicates the mapped region, lower left (LL) and upper right (UR) corners of stiffness maps (relevant to **c** and **f**) are indicated, the colours indicate areas selected for regional analysis (relevant to **g** and **h**). **c,** AFM-based stiffness maps (colour maps), encoding the apparent elastic modulus, *K*, a measure of tissue stiffness, assessed at an indentation force *F* = 10 nN for control or Piezo1 downregulation exclusively in axons, in the surrounding brain tissue, or both. **d,** Quantification of AFM experiments. Downregulating Piezo1 in the brain parenchyma resulted in significant tissue softening.

Violin plots with scatter of individual stiffness measurements for each condition. The means and medians are indicated as yellow crosses and white squares, respectively. Data was assessed with a Kruskal-Wallis test, $p < 0.0001$, followed by Dunn post-hoc tests (adjusted p-values provided in the figure). **e,** Exposed brain preparation of a stage 40 *Xenopus* embryo electroporated with fluorescein-tagged morpholinos, enabling the visualisation of the electroporated region. The dotted white line shows the whole brain and the dotted blue line highlights the electroporated region. (**f-h**) Downregulating Sema3A does not cause brain tissue softening. **f,** AFM-based stiffness maps (colour maps) for control or Sema3A morpholino-electroporated brains. **g-h,** Violin plots with scatter of individual stiffness measurements for each condition. Data were assessed with a Wilcoxon rank sum test. **g,** The electroporated regions were significantly stiffer in the Sema3A KD compared with the controls whereas **h,** the adjacent regions were mechanically similar. Scale bars: 100 µm. N denotes the number of animals, n denotes the number of measurements. KD: knockdown.

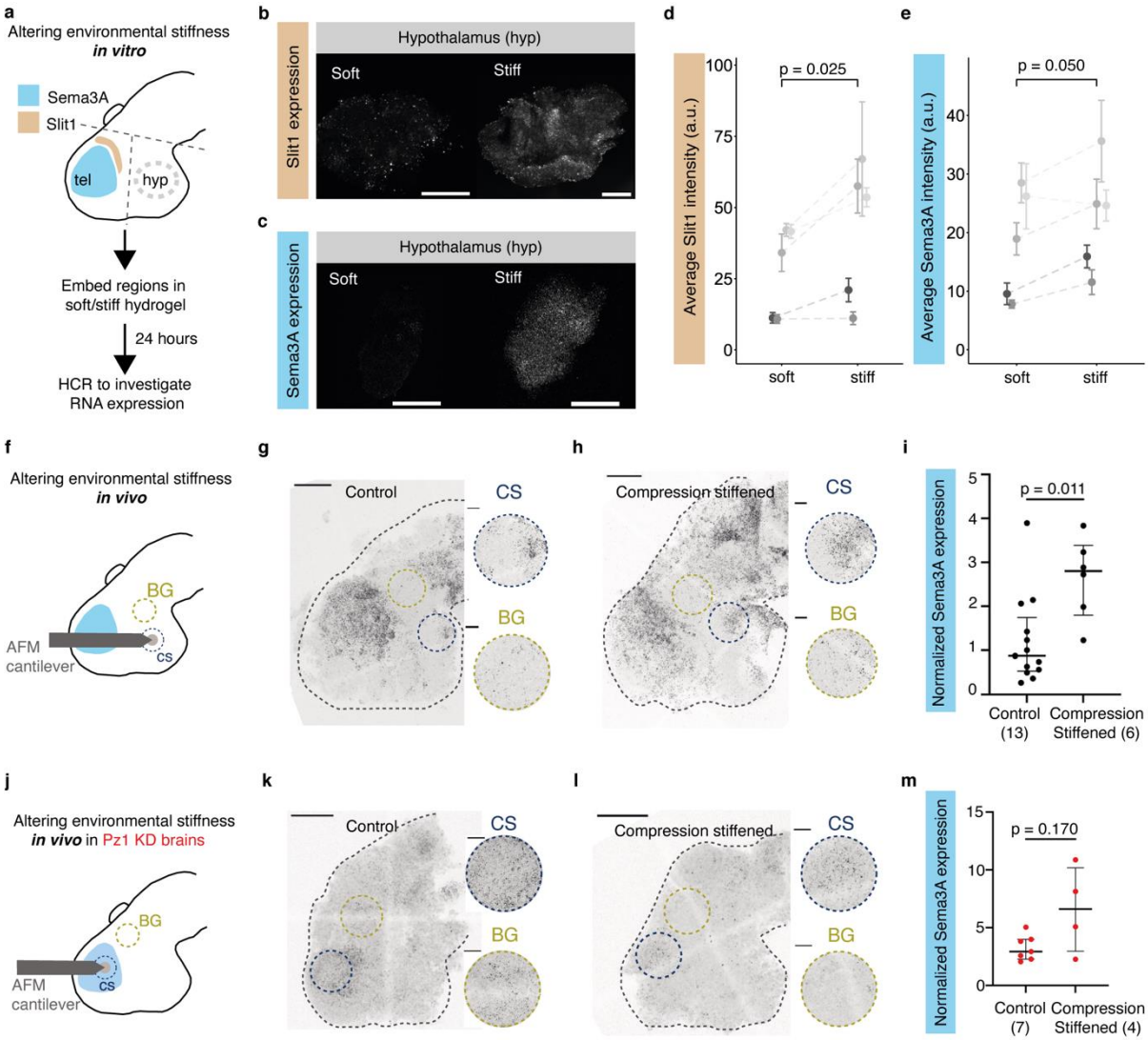

Figure 4: Altering stiffness *in vitro* and *in vivo* affects chemical guidance cue expression. a, Schematic of the experimental setup for perturbing environmental stiffness *in vitro*. The telencephalon and hypothalamus regions, were dissected (dashed lines) and embedded in soft or stiff 3D substrates. HCR-FISH was used to quantify Slit1 and Sema3A mRNA expression after 24 hours. **b-c,** Representative images of Slit1 (**b**) and Sema3A (**c**) expression in hypothalamic tissue embedded in soft and stiff substrates. **c,** Representative images of expression in the hypothalamus in soft (left) and stiff (right) substrates. **d-e,** Quantification of mRNA expression. Both Slit1 (**d**) and (**e**) Sema3A expression increased significantly in stiffer environments. Points represent means of a biological replicate. Ratio

paired t-tests were used to test for statistical analysis. **f,** Schematic of the experimental setup for locally increasing tissue stiffness in wild type brains *in vivo.* The hypothalamus region of the brain was compression-stiffened with a sustained force of 30-40 nN applied with an AFM probe of ~90-120 µm diameter for > 6 hours. **g-h,** Representative images of Sema3A HCR-FISH in control and compression-stiffened brains. The insets show representative regions which were selected for analysis. **i,** The ratio of the total area covered by signal in the compression-stiffened (CS) region to the mean area covered by the signal in background (BG) regions were analysed. Sema3A expression significantly increased in compression-stiffened hypothalamic brain regions compared with control brains. **j,** Schematic of the experimental setup for perturbing tissue stiffness in Piezo1 knockdown brains *in vivo*. The telencephalic region of the brain was compression-stiffened as in (**f**). **k-l,** Representative images of Sema3A HCR-FISH in control and compression-stiffened Piezo1 knockdown brains. The insets show representative regions which were selected for analysis. **m,** Sema3A expression did not change in response to the applied force. Unpaired t-tests with Welch's correction were used for statistical analysis, number of animals in parentheses. Each point refers to an embryo. Scale bars in whole brain images: 100 µm; scale bars in insets: 20 µm. hyp: hypothalamus, KD: knockdown, tel: telencephalon.